J|A|C|S
COMMUNICATIONS

Published on Web 08/23/2002

A Metal−Organic Bilayer Open Framework with a Dynamic Component: Single-Crystal-to-Single-Crystal Transformations

Myunghyun Paik Suh,* Jung Woo Ko, and Hye Jin Choi

School of Chemistry and Molecular Engineering, and the Center for Molecular Catalysis,
Seoul National University, Seoul 151-747, Republic of Korea

Received November 17, 2001; Revised Manuscript Received July 29, 2002

Metal−organic open frameworks assembled from designed molecular building blocks may be applied to adsorption and separation processes,[1−3] ion-exchange,[4,5] catalysis,[6,7] and sensor technology.[8,9] Compared with the formation of inorganic porous materials such as zeolites, modular construction of these frameworks allows control of size, shape, and chemical environment of the voids.[10−12] Retaining single-crystallinity even after chemical reactions is also important for certain devices.

Here we report the synthesis of a bilayer open framework, which retains its framework and the single-crystallinity upon removal and exchange of the guest molecules. The crystal even shows spongelike dynamic behavior, reducing the interlayer spacing dramatically in response to guest removal. This type of crystal dynamic is unprecedented although some metal−organic frameworks retained crystallinity upon guest loss.[1,12−14] Our synthetic strategy was based on the construction of 3D channels in a bilayer framework consisting of robust 2D nickel(II) layers and flexible pillars.

The bilayer open framework (**BOF-1**), where metal−organic 2D layers are held together by the covalent bonds, was assembled from dinickel(II) bismacrocyclic complex $[Ni_2(C_{26}H_{52}N_{10})(Cl)_4]\cdot H_2O$ (**A**) (Figure 1) and sodium 1,3,5-benzenetricarboxylate (Na_3BTC) in water in the presence of DMSO and pyridine. Nickel(II) macrocyclic complexes in square-planar geometry are useful in design and synthesis of multidimensional networks since they have two fixed vacant coordination sites (trans).[15,16] **A** was prepared from formaldehyde, *N*,*N′*-bis(2-aminoethyl)-1,3-propanediamine, and *p*-xylylenediamine, by modifying one-pot metal-template condensation reactions.[17,18]

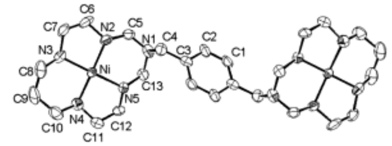

Figure 1. X-ray structure of dinickel(II) bismacrocyclic complex in $[Ni_2(C_{26}H_{52}N_{10})](PF_6)_4\cdot 2H_2O$ (**A-PF₆**).

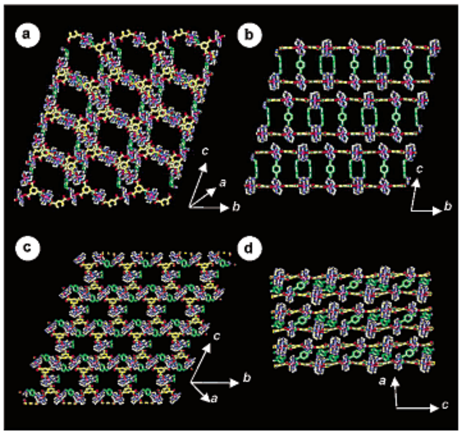

Figure 2. X-ray structures of **BOF-1**. (a) Top view of **1**, showing 2D layers of brick-wall motif. (b) Side view of **1**, showing pillared-bilayer structure (thickness of bilayer, 11.91(1) Å). (c) Top view of desolvated crystal **2**. (d) Side view of **2** showing tilted pillars (thickness of bilayer, 6.82(2) Å). Ni, pink; O, red; N, blue; C of macrocycle, gray; C of BTC^{3-}, yellow; C of pillars, green. Guest water and pyridine molecules are omitted for clarity.

The X-ray crystal structure of **BOF-1** as prepared, $[Ni_2(C_{26}H_{52}N_{10})]_3[BTC]_4\cdot 6C_5H_5N\cdot 36H_2O$ (**1**) (0.4 × 0.4 × 0.1 mm³), was determined at 100 K in a sealed glass capillary filled with mother liquor since the crystal loses guest molecules upon exposure to the atmosphere.[19] In **1**, each nickel(II) macrocyclic unit of **A** is coordinated by two BTC^{3-} ions at the trans position, and each BTC^{3-} ion binds three nickel(II) ions belonging to three different bismacrocyclic units, which results in two 2D layers with the brick-wall motif of size 22.6 × 14.3 Å² (Figure 2a). The *p*-xylyl groups of the bismacrocycle act as pillars to hold two layers together (Figure 2b). The assembly did not show architectural isomerism that might yield a 3D network locating **A** alternately in 2D layers.[20] The thickness of the bilayer is 11.91(1) Å. The open-framework creates 3D channels, as seen in Figure 2, which are filled with water and pyridine guest molecules. The channel walls created on the side of the bilayer are made of *p*-xylyl pillars. The rings of *p*-xylyl groups are positioned regularly almost parallel and perpendicular to the direction of the side channels (with the dihedral angles of 1.40°, 87.9°, and 88.4° between them). The channel width seen on the side of the bilayer is 14.52(1) Å (the effective channel width corrected for van der Waals surface is 11.12(1) Å). The void volume of the channels is estimated to be 61% of the total volume. Thermogravimetric analysis of **1** indicates that all guest molecules can be removed at 133 °C and that the solid is stable up to 275 °C.

When a single crystal **1** was allowed to stand in air for 2 h, all pyridine and some water guest molecules were removed to yield $[Ni_2(C_{26}H_{52}N_{10})]_3[BTC]_4\cdot 30H_2O$ (**1′**). The X-ray structure of **1′** (Supporting Information) indicates that the cell volume and thickness of bilayer are reduced compared with those of **1** (Table 1).

When crystal **1** (0.2 × 0.2 × 0.1 mm³) was taken from the capillary after the cell parameters were measured and then dried at 75 °C for 1.5 h in a furnace, the transparency was slightly lost, and $[Ni_2(C_{26}H_{52}N_{10})]_3[BTC]_4\cdot 4H_2O$ (**2**) resulted.[21] The crystal **2** was immediately protected from the moisture of the air with epoxy resin, and the X-ray structure was determined (Figure 2c,d). The cell parameters including the cell volume changed significantly during the transformation from **1** to **2** (Table 1), but the single-crystallinity was still retained. In **2**, no practical change was observed in the 2D layers (the cavities of size 22.2 × 14.4 Å²), but the thickness of the bilayer was greatly reduced to 6.82(2) Å, due to significant tilting of the pillars. In contrast to intuitive view, a spongelike crystal

---

* To whom correspondence should be addressed. E-mail: mpsuh@snu.ac.kr.

10.1021/ja017560y CCC: $22.00 © 2002 American Chemical Society

Table 1. Crystallographic Parameters for **1**−**4**[a]

compound	**1**	**1′**	**2**	**3**	**4**
space group	$P\bar{1}$	$P\bar{1}$	$P1$	$P\bar{1}$	$P\bar{1}$
a, Å	16.505	16.420	12.382	16.467	16.460
b, Å	19.945	19.817	16.375	20.134	19.849
c, Å	20.664	20.439	19.952	20.720	20.419
α, deg	73.00	70.32	74.51	72.53	70.50
β, deg	68.24	68.55	89.26	67.94	71.08
γ, deg	76.07	76.19	84.18	75.04	76.30
V, Å^3	5974.3	5777.9	3877.9	5990.4	5887.0
thickness of bilayer, Å	11.91(1)	11.27(2)	6.82(2)	11.71(1)	11.75(2)

[a] R_1 (unweighted, based on F^2) values are 0.0899 for **1**, 0.1839 for **1′**, 0.1491 for **2**, 0.1279 for **3**, 0.1299 for **4**.

Table 2. Guest Binding Data for Dried **BOF-1**[a,b]

	K_f, M^{-1}	$[BS]_o/\omega$, mmol g^{-1}	guest inclusion capacity[c], mol
MeOH	4.61 ± 1.82	10.5 ± 1.34	29.1
EtOH	4.55 ± 1.31	5.35 ± 0.50	14.8
iso-PrOH	6.49 ± 3.88	2.11 ± 0.58	5.84
BzOH	18.8 ± 8.54	1.31 ± 0.19	3.62

[a] Measurements were performed according to the method in ref 16. [b] K_f and $[BS]_o/\omega$ indicate the binding constant and the binding capacity of host solid with guest molecules, respectively. [c] Per formula unit of host **2**.

dynamic took place in response to the loss of guest molecules without breaking the single-crystallinity. The void volume of **2** is 27% of the total volume.[22] When the single crystal **2** was exposed to water−pyridine vapor for 12 h or immersed in water−pyridine mixture for 5 min, it restored structure **1** as evidenced by X-ray powder diffraction patterns (see Supporting Information) although the crystal was split into pieces that are too small to determine the X-ray structure again.

The dried compound **2**, which was ground into powder, differentiates various alcohols in toluene, showing Langmuir isotherm curves (see Supporting Information). The binding constants (K_f) and the maximum number of binding sites for the guest molecules per gram of host solid ($[BS]_o/\omega$) are summarized in Table 2.

We also examined the guest-exchange processes for the crystal **1** with pyridine and benzene, in which **1** was completely insoluble.[23] When single-crystal **1**, whose cell parameters were measured, was immersed in pyridine within a glass capillary (0.5 mm i.d.) for 24 h, the X-ray structure determined at 100 K indicated that some water guest molecules in **1** were exchanged with pyridine to result in $[Ni_2(C_{26}H_{52}N_{10})]_3[BTC]_4\cdot 20C_5H_5N\cdot 6H_2O$ (**3**).[24,25] Similarly, when single-crystal **1** was immersed in benzene within a capillary for 24 h, the structure determined at room temperature indicated that some of the guest molecules in **1** were exchanged with benzene to result in $[Ni_2(C_{26}H_{52}N_{10})]_3[BTC]_4\cdot 14C_6H_6\cdot 19H_2O$ (**4**).[24,25] During the guest-exchange processes, crystal-to-crystal conversion also took place, retaining the transparency of the crystal. The cell parameters in **3** and **4** are almost the same as in **1** (Table 1). The crystal structures of **3** and **4** are shown in Figure 3. It should be noted that the R_1 values are extraordinarily high, 0.1279 for **3** and 0.1299 for **4**. In **3**, pyridine molecules are included in the channels of the framework via face-to-edge $\pi-\pi$ interactions with the phenyl rings of BTC^{3-} of the 2D layers and with the aromatic ring planes of the pillars. They are also intercalated between the bilayer units via hydrogen-bonding interactions with the host. In **4**, benzene molecules are included only in the channels by the $\pi-\pi$ interactions with the host. The size of the brick-wall motif in 2D and the thickness of the bilayer in **3** and **4** were unaltered relative to those of **1**.

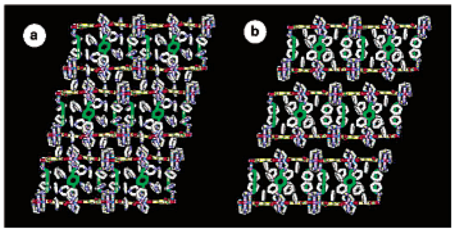

Figure 3. X-ray structures of **3** and **4**. (a) Side view of **3**. (b) Side view of **4**. The colors are the same as in Figure 2. Organic guest inclusions are indicated as off-white, and water guest molecules are omitted for clarity.

In conclusion, **BOF-1**, a pillared-bilayer framework with 3D channels, shows dynamic behavior in response to amount of guest. It exhibits crystal-to-crystal transformation upon the guest removal and the exchange processes. The design may be applied to prepare a new class of versatile multifunctional crystalline materials.

Acknowledgment. This work was supported by the Korea Science and Engineering Foundation (Basic Research Program 2000-2-12200-002-1) and Center for Molecular Catalysis.

Supporting Information Available: Detailed experimental procedures, ORTEP drawing of **1**, X-ray structure of **1′**, XRPD patterns, guest binding curves, photographs for guest exchange processes, and Tables for X-ray data of **A-PF$_6$** and **1**−**4** (PDF). An X-ray crystallographic file (CIF). This material is available free of charge via the Internet at http://pubs.acs.org.

References

(1) Li, H.; Eddaoudi, M.; O'Keeffe, M. Yaghi, O. M. *Nature* **1999**, *402*, 276.
(2) Noro, S.-I.; Kitagawa, S.; Kondo, M.; Seki, K. *Angew. Chem., Int. Ed.* **2000**, *39*, 2082.
(3) Choi, H. J.; Lee, T. S.; Suh, M. P. *Angew. Chem., Int. Ed.* **1999**, *38*, 1405.
(4) Min, K. S.; Suh, M. P. *J. Am. Chem. Soc.* **2000**, *122*, 6834.
(5) Yaghi, O. M.; Li, H. *J. Am. Chem. Soc.* **1996**, *118*, 295.
(6) Seo, J. S.; Whang, D.-M.; Lee, H.-Y.; Jun, S. I.; Oh, J.-H.; Jeon, Y.-J.; Kim, K.-M. *Nature* **2000**, *404*, 982.
(7) Sawaki, T.; Aoyama, Y. *J. Am. Chem. Soc.* **1999**, *121*, 4793.
(8) Albrecht, M.; Lutz, M.; Spek, A. L.; van Koten, G. *Nature* **2000**, *406*, 970.
(9) Real, J. A.; Andrés, E.; Muñoz, M. C.; Julve, M.; Granier, T.; Bousseksou, A.; Varret, F. *Science* **1995**, *268*, 265.
(10) Yaghi, O. M.; Li, H.; Davis, C.; Richardson, D.; Groy, T. L. *Acc. Chem. Res.* **1998**, *31*, 474.
(11) Chui, S. S.-Y.; Lo, S. M.-F.; Charmant, J. P. H.; Orpen, A. G.; Williams, I. D. *Science* **1999**, *283*, 1148.
(12) Chen, B.; Eddaoudi, M.; Hyde, S. T.; O'Keeffe, M.; Yaghi, O. M. *Science* **2001**, *291*, 1021.
(13) Biradha, K.; Hongo, Y.; Fujita, M. *Angew. Chem., Int. Ed.* **2000**, *39*, 3843.
(14) Kepert, C. J.; Rosseinsky, M. J. *Chem. Commun.* **1999**, 375.
(15) Choi, H. J.; Suh, M. P. *J. Am. Chem. Soc.* **1998**, *120*, 10622.
(16) Min, K. S.; Suh, M. P. *Chem. Eur. J.* **2001**, *7*, 303.
(17) Suh, M. P. *Adv. Inorg. Chem.* **1996**, *44*, 93.
(18) Suh, M. P.; Kim, S. K. *Inorg. Chem.* **1993**, *32*, 3562.
(19) Due to the loss of guest molecules in air, the XRPD pattern of crystal **1** ground in air is almost same as that of air-dried sample (**1′**) (see Supporting Information).
(20) Holman, K. T.; Martin, S. M.; Parker, D. P.; Ward, M. D. *J. Am. Chem. Soc.* **2001**, *123*, 4321.
(21) When crystal **1** was dried up to 135 °C at the rate of 3.8 °C/min, it did not diffract the X-ray beam. However, the single-crystal dried at 100 °C (heating rate, 1.5 °C/m) shows $a = 11.948(9)$ Å, $b = 16.108(15)$ Å, $c = 19.553(24)$ Å, $\alpha = 74.66(5)°$, $\beta = 88.53(5)°$, $\gamma = 84.46(3)°$, $V = 3612.0(6)$ Å^3.
(22) N_2 gas sorption results: Langmuir surface area, 138 m^2/g; pore volume, 0.0876 cm^3/g.
(23) Insolubility was checked by NMR spectra measured with the d_5-pyridine and d_6-benzene solutions after crystals **1** were immersed for 24 h, which showed no peak corresponding to the framework of **1**.
(24) The possibility of dissolution of **1** in the solvents followed by crystallization of **3** and **4** is excluded by the photographs taken under an optical microscope during and after the immersion, which showed no change in size, morphology, transparency, and position of the crystal (see Supporting Information).
(25) Detailed methods are described in Supporting Information.

JA017560Y